Applied Catalysis A: General 515 (2016) 164–169

Contents lists available at ScienceDirect

Applied Catalysis A: General

journal homepage: www.elsevier.com/locate/apcata

Synthesis of conjugated Mn porphyrin polymers with *p*-phenylenediamine building blocks and efficient aerobic catalytic oxidation of alcohols

Yongjin Li, Baoshuai Sun, Weijun Yang*

Department of Chemistry and Chemical Engineering, Hunan University, Changsha, 410082 Hunan, China

ARTICLE INFO

Article history:
Received 27 October 2015
Received in revised form 31 January 2016
Accepted 5 February 2016
Available online 8 February 2016

Keywords:
N-Heterocyclic carbene
Aromatic amination
Conjugated metalloporphyrin polymer
Alcohol oxidation
Catalysis

ABSTRACT

A series of conjugated metalloporphyrin polymers (MnP-AMPs) were synthesized based on Buchwald-Hartwig aromatic amination with *p*-phenylenediamine and manganese tetraphenylporphyrin as building blocks, and N-heterocyclic carbene-palladium complex as catalyst. Brunauer–Emmett–Teller surface area analysis, scanning electron microscopy and transmission electron microscopy showed that MnP-AMPs had large surface areas and uniform pore sizes. The stable porous and superreticular conjugated structure of MnP-AMP further activated manganese ions in the porphin ring compared with those in the original monomanganeseporphyrin. Moreover, introducing C—N bonds in MnP-AMP increased its polarity and affinity to alcohols, so MnP-AMP exhibited high catalytic activity when applied to aerobic oxidation of alcohols. For the catalysis of selective oxidation of benzyl alcohol to benzaldehyde with air, the conversion and aldehyde selectivity both reached up to 100% under mild condition in acetonitrile at 40 °C. MnP-AMP also remained stable in oxidation reaction system and still had high catalytic activity after several recycles.

1. Introduction

Metalloporphyrins, as excellent biomimetic catalysts for C—H bond activation [1,2], can also be used in catalytic oxidation of alcoholic hydroxyl group with high selectivity [3,4]. However, they are generally responsible for catalysis in homogeneous systems and prone to self-oxidation and degradation, rendering recycle and reuse rather difficult [5]. The existing problems can mainly be solved by utilizing metalloporphyrins in a multiphase process, immobilization in most cases [6–8]. New bonds form in metalloporphyrin immobilization, which are generally unstable and easily breakable, so the performance in reuse is limited [9]. Self-oxidization, degradation, or difficulty in reuse cannot be circumvented by metalloporphyrin immobilization [10]. Aggregating metalloporphyrin to special insoluble polymer is a new method for the heterogeneous catalysis of metalloporphyrins [11–13].

Metalloporphyrin polymerization can be mainly divided into four categories: hydrogen-bonding association [14,15], axial polymerization [16], metal-organic frameworks [17,18], and para-covalent polymerization [19,20]. Para-covalent polymerization connects metalloporphyrin monomers through covalent bonds. Such polymers can form different kinds of covalent polymers by changing the coupling groups [21,22]. Since para-covalent polymerization hardly occurs in four para positions of metalloporphyrin, only phenylene- and alkynyl-coupling conjugated polymers have been successfully synthesized till now [23,24]. Synthesis of phenylimine-coupling metalloporphyrin polymer and application of it in the catalytic oxidation of alcohol have not been reported yet. In this study, we designed a conjugated metalloporphyrin polymer coupled with phenylimine, which had a porous network structure with hyperconjugation, further activating center manganese ions compared with those in monometalloporphyrin. A large number of C—N bridging groups enhanced the polarity of the polymer, so it showed high affinity to alcohols and superb catalytic performance for the oxidation of alcohols into aldehydes.

The coupling reaction between phenylimine and metalloporphyrin polymer could not be catalyzed by common palladium catalysts such as tetrakis(triphenylphosphine) palladium(0), $Pd(dba)_2$, and tetrakis (triphenylphosphine) palladium(0)/CuI. N-Heterocyclic carbene palladium complex is a new coupling catalyst for Buchwald-Hartwig aromatic amination [25,26]. *N*,*N*-(2,4,6)-Methylimidazolium chloride, a N-heterocyclic carbene precursor, was herein synthesized. It exhibited high catalytic activity when combined with palladium acetate in four-directional coupling polymerization with *p*-phenylenediamine and T(p-Br)PPMnCl.

* Corresponding author.
E-mail address: wjyang@hnu.edu.cn (W. Yang).

http://dx.doi.org/10.1016/j.apcata.2016.02.003
0926-860X/

2. Experimental

2.1. Reaction reagents

Palladium acetate (47.5% Pd) and potassium *tert*-butoxide (95%) were obtained from J&K Chemicals. (p-Br)PPMnCl was synthesized in our group according to documented procedures and characterized by IR, UV–vis, ^{1}H NMR and MS spectroscopies [27] (Supporting information). *P*-Phenylenediamine, chloromethyl ethyl ether and other reagents were purchased from Alfa Aesar Corp. and Aldrich Corp., and were all analytical grades without special treatment.

2.2. Synthesis of $(Pd(IMes)Cl_2)_2$ catalyst

2.2.1. Synthesis of glyoxal-bis (2,4,6-trimethylphenyl)-imine

Typical procedures: 2,4,6-Trimethylaniline (2.7042 g, 0.02 mmol) and *n*-propanol (12 mL) were added to a three-neck flask, into which a mixture of 40% glyoxal (0.01 mol, 1.4510 g), 8 mL *n*-propanol and 4 mL water was then slowly added. After 4 h of reaction at 25 °C and another 2 h of reaction at 60 °C, the reactants were removed into ice water to allow full evaporation. The precipitate was collected by filtration, thoroughly washed with *n*-propanol and then dried in vacuum with a yield of 71.2% (2.0790 g). The products were identified on the basis of ^{1}H NMR and ^{13}C NMR spectral data.

^{1}H NMR ($CDCl_3$): δ 2.19 [s, 12H, *ortho*-CH_3], 2.32 [s, 6H, *para*-CH_3], 6.93 [s, 4H, *meta*-CH], 8.13 [s, 2H, CH]. ^{13}C NMR ($CDCl_3$): δ 18.2 [s, *ortho*-CH_3], 20.7 [s, *para*-CH_3], 126.5 [s, *ortho*-C], 128.9 [s, *meta*-C], 134.1 [s, *para*-C], 147.4 [s, *ipso*-C], 163.0 [s, HC=N].

2.2.2. Synthesis of IMes·HCl

Typical procedures: The above obtained glyoxal-bis(2,4,6-trimethylphenyl)-imine (0.4382 g, 1.50 mmol) was added to a three-neck flask, degassed by three freeze-pump-thaw cycles, and purged with argon. Afterwards, 5 mL THF was added to the flask via a syringe until the solid completely dissolved at 45 °C. Then chloromethyl ethyl ether and 1 mL THF were dropwise added to the flask after the temperature was cooled to 15 °C. Finally, the reactants were stirred at 20 °C for 1 h. After reaction, the precipitate was collected by filtration, thoroughly washed with THF and then dried in vacuum with a yield of 62.0% (0.3169 g). The obtained solid was characterized as N,N-(2,4,6-trimethylphenyl) imidazolium chloride (IMes·HCl) on the basis of ^{1}H NMR spectral data.

^{1}H NMR ($CDCl_3$): δ 2.08 [s, 12H, *ortho*-CH_3], 2.27 [s, 6H, *para*-CH_3], 6.95 [s, 4H, *meta*-CH], 7.61 [s, 2H, im-$H^{4,5}$], 10.06 [s, 1H, im-H^2].

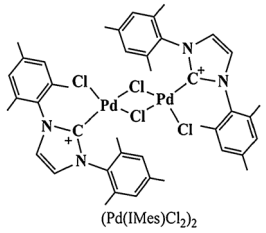

Fig. 1. Structure of $(Pd(IMes)Cl_2)_2$.

2.2.3. Synthesis of $(Pd(IMes)Cl_2)_2$ catalyst

Potassium *tert*-butoxide (33.6 mg, 0.30 mmol), potassium chloride (44.7 mg, 0.60 mmol), palladium acetate (27.0 mg, 0.12 mmol) and IMes·HCl (102.0 mg, 0.30 mmol) were added to a three-neck flask which had been purged thoroughly with argon. Deoxygenated, anhydrous THF (12 mL) was added via a syringe under stirring, and the solution was heated at reflux for 16 h after all the reaction reagents dissolved. After reaction, the solution was evaporated under argon at 30 °C, and the orange red solid complex was purified by silica gel chromatography (Et_2O/hexanes, 1:1) with a yield of 38%. The products were identified on the basis of ^{1}H NMR, ^{13}C NMR and MS spectral data (Fig. 1).

$(Pd(IMes)Cl_2)_2$: MS: *m*/*z* 964; ^{1}H NMR ($CDCl_3$): *δ* 6.85 [s, 4H], 6.13 [s, 4H], 2.31 [s, 12H], 2.05 [s, 24H]; ^{13}C NMR ($CDCl_3$): δ 18.5 [ortho-CH_3], 21.6 [para-CH_3], 121.3 [C=C], 127, 136.1, 136.9, 137.3 [aryl-C], 195.3 [N—C—N]; Elemental analyses: C, H, Cl, N and Pd was 52.45, 4.98, 14.65, 5.88, and 22.04 wt% respectively.

2.3. Synthesis of MnP-AMP

A mixture of $(Pd(IMes)Cl_2)_2$ (96.4 mg, 0.10 mmol), T(p-Br)PPMnCl (100.2 mg, 0.10 mmol), *p*-phenylenediamine (27.0 mg, 0.25 mmol), potassium *tert*-butoxide (56.0 mg, 0.50 mmol) and anhydrous m-xylene (8 mL) was added to a reaction flask, degassed by three freeze-pump-thaw cycles, purged with argon, and stirred

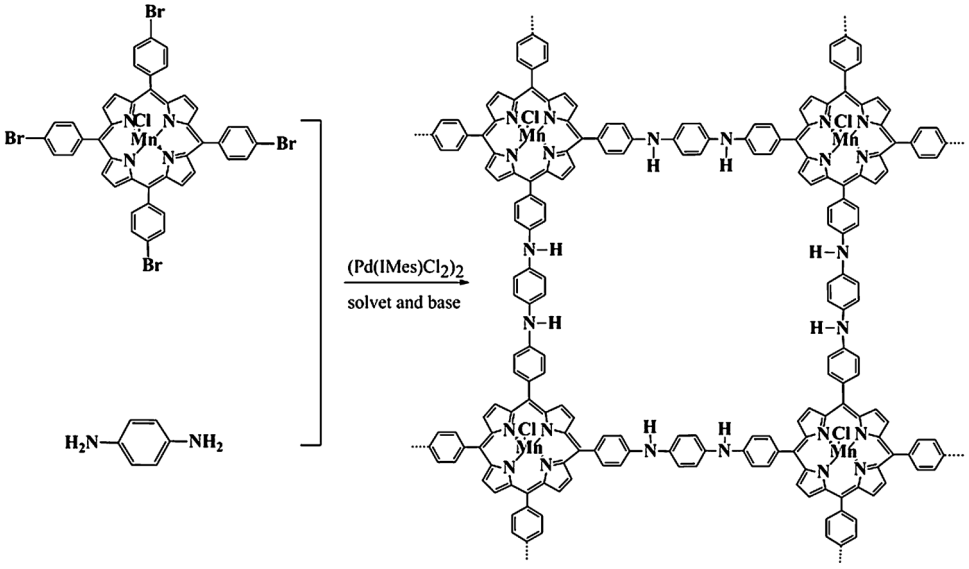

Fig. 2. Schematic representation of the synthesis of MnP-AMP.

at 135 °C for 24 h. Finally, the mixture was allowed to cool at room temperature, into which ethanol was added. The precipitate was collected by filtration, thoroughly washed with water/ethanol, trichloromethane respectively, and then dried in vacuum to give MnP-AMP as a black solid in 86.1% isolated yield. (Fig. 2.).

2.4. Methods of polymer characterization

MnP-AMP was further purified by Soxhlet extraction for 24 h with ethanol and trichloromethane before test.

FT-IR spectrum was measured by Fourier Transform Infrared Spectrometer (IRrestige-21, Shimadzu). The sample was completely dried and diluted by potassium bromide as a pretreatment.

The specific surface areas and pore size distribution were detected by Micromeritics TriStar II 3020 accelerated surface and porosity analyzer with nitrogen as probing gas at 77 K. Before measurement, samples were degassed and fully dried in vacuum at 120 °C for more than 12 h. The specific surface areas were calculated by the Brunauer–Emmett–Teller (BET) method, and the NFT theory was utilized to estimate pore size, pore volume and pore distribution.

Field emission scanning electron microcopies (FE SEM) were performed by a JEOL model JSM-6400F microscope. High resolution transmission electron microcopies (HR TEM) were performed by a JEOL model JEM-3010 microscope.

The UV–vis diffuse reflectance spectra of MnP-AMP was measured on an Agilent Technologies model Cary 100 UV–vis spectrophotometer equipped with integration sphere, and the samples were diluted with $BaSO_4$.

Elemental analyses of C, H, N were carried out on an German Elementar corporation model vario ELIII. Elemental analyses of Pd were carried out by atomic absorption spectrometry on America Perkin Elmer model Aanalyst 700/800.

2.5. Cyclic voltammetry of the polymer

Electrochemical measurements of cyclic voltammetry had been investigated using a CHI66OB electrochemical workstation with a three-electrode cell system, in which a glass carbon after loading the MnP-AMP was used as the working electrode, a calomel electrode as the reference electrode, and a Pt wire as the counter electrode. As to electrode preparation, the sample MnP-AMP was dispersed in 0.5 mL solvent mixture containing 11 μL of nafion (5 wt%) and 0.49 mL of ethanol by sonication for more than 1 h to obtain the stable suspension. And then 10 μL portion of the sample solution was slightly dropped on the surface of the pre-polished gassy carbon electrode. The electrodes were dried overnight at room temperature for measurement. The electrochemical experiments were conducted in 0.1 mol/L $(CH_3CH_2)_4NBr$ CH_2Cl_2 solution. The experiments were cyclically scanned at a scan rate of 50 mV/s at the room temperature after purging Ar gas for 10 min.

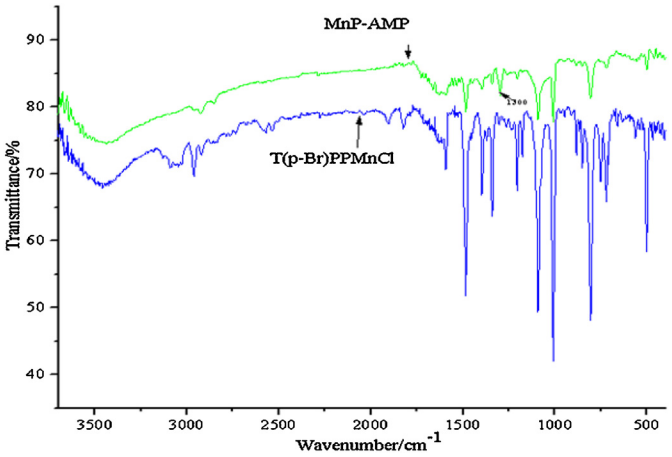

Fig. 3. FT-IR spectra of MnP-AMP and T(p-Br)PPMnCl.

2.6. Catalytic oxidation of alcohols

Alcohols (3.0 mmol), MnP-AMP catalyst (3.0×10^{-3} mmol) and acetonitrile (8 mL) were added to a three-neck flask, into which isobutyraldehyde (9.0 mmol) was also dropped in three portions (3.0 mmol each time) with stirring. The temperature and the air flow rate were maintained at 40 °C and 150 mL/min respectively. The reaction time was 2–6 h.

3. Results and discussion

3.1. MnP-AMP characterization

As shown in Fig. 3, the IR spectrum of T(p-Br)PPMnCl exhibits a characteristic Mn-N vibration band at 1010.9 cm^{-1}, which is close to that of MnP-AMP (1009.1 cm^{-1}). The peaks at 1516 cm^{-1} and 1608 cm^{-1} correspond to C=C stretches in phenyls respectively, and that at 600 cm^{-1} represents C-Br in porphyrin. Different from that of T(p-Br)PPMnCl, the characteristic peak of C-Br in MnP-AMP at 600 cm^{-1} attenuates and even disappears due to consumption of C-Br during the coupling reaction. MnP-AMP is a conjugated poly-

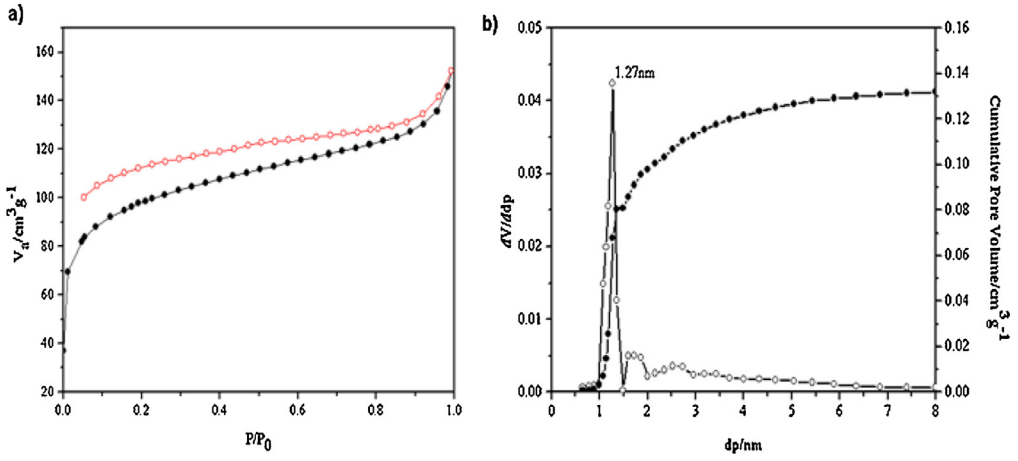

Fig. 4. (a) Nitrogen adsorption (●) and desorption (○) isotherm profiles of MnP-AMP at 77 K. (b) Pore size distribution (○) and cumulative pore volume (●) of MnP-AMP.

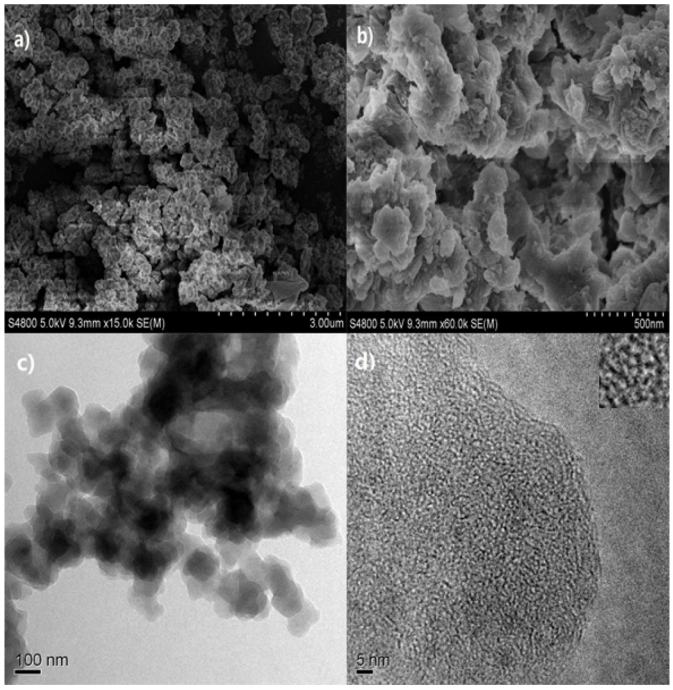

Fig. 5. (a, b) FE SEM and (c and d) HR TEM images of MnP-AMP.

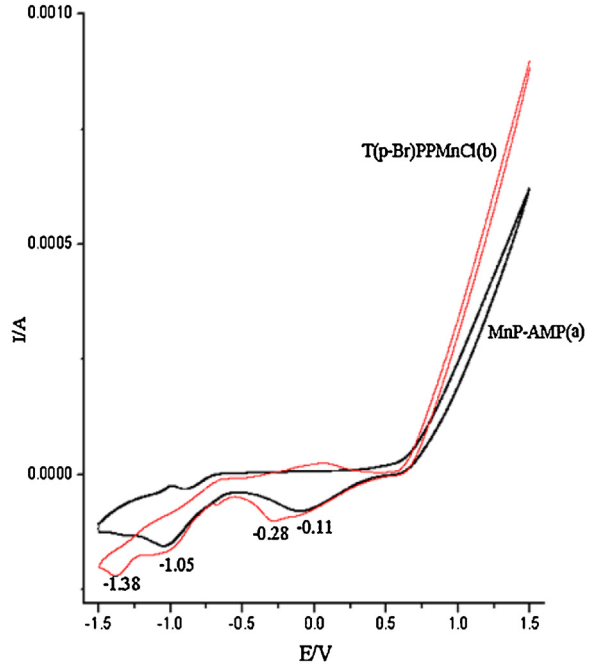

Fig. 6. (a) Cyclic voltammetry curves of MnP-AMP on the glass carbon electrodes in 0.1 mol/L $(CH_3CH_2)_4NBr$ CH_2Cl_2 solution (black curve); (b) cyclic voltammetry curves of T(p-Br)PPMnCl in CH_2Cl_2, 0.1 mol/L $(CH_3CH_2)_4NBr$ (red curve). Scan rate is 50 mV/s. (For interpretation of the references to color in this figure legend, the reader is referred to the web version of this article.)

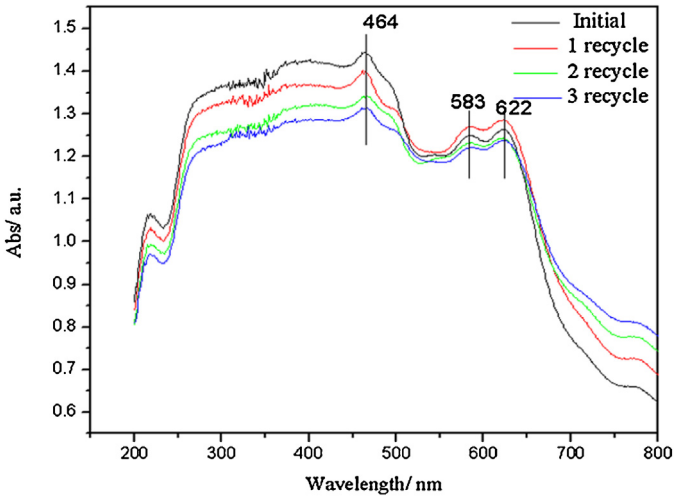

Fig. 7. The UV–vis diffuse reflectance spectra of MnP-AMP.

mer with metalloporphyrin and ursol building blocks, in which the lone electron-pair of N atom conjugates with benzene ring, making C—N show double-bond properties. Given the new peak at 1300 cm^{-1}, the coupling reaction was successful. N—H bond exhibits a very weak absorption peak at 3300–3500 cm^{-1}.

The sorption curve of MnP-AMP at 77 K (Fig. 4a) is a typical type-II sorption and a type-S sorption isotherm plot, exhibiting a strong adsorption at low pressure ($P/P_0 < 0.1$). In addition, micro- and mesopores coexisted in the framework. The BET surface area was as high as 345 m^2g^{-1}, of which the micro-pore area (about 197 m^2g^{-1}) accounted for 57.1%. The main pore diameters were about 1.27 nm (Fig. 4b), and these pores (about 0.226 cm^3g^{-1}) contributed to 38.2% of the pore volume based on the cumulative pore volume profile. Therefore, MnP-AMP was an excellent micro- and mesoporous polymer.

FE SEM images (Fig. 5a and b) show that MnP-AMP has a columnar structure accumulated by porphyrin layers among which there is network interpenetration. Moreover, these layers were diametered about 100–200 nm and irregularly sized, which led to an unequal columnar distribution. As shown in HR TEM images (Fig. 5c), these lamellar layers are diametered about 100 nm. According to the high-magnification image (Fig. 5d), there are a large number of about 1.0 nm nanoholes on the surface of MnP-AMP, being consistent with the pore size analysis results.

The first reduction potential of MnP-AMP was significantly reduced compared with the first reduction potential of T(p-Br)PPMnCl (from −0.28 V right shift to −0.11 V), which indicated that the structure of -NH-Ar- was introduced into the polymers (Fig. 6). And the structure of -Ar-NH-Ar-NH-Ar- as conjugated bridges between the porphyrin monomers was advantageous to the electron flow to from lively valence ions, and made the reduction of the metal more easily.

The UV–vis diffuse reflectance spectra of the polymers before and after the oxidation reaction were also measured (Fig. 7). The UV–vis diffuse reflectance spectra have no evident changes before and after the oxidation reaction even for more than three recycle uses. In the curves, the absorption band at 464 nm is the Soret band, and those at 583 and 622 nm are the Q-bands of the Mn-porphyrin units of MnP-AMP. Moreover, the UV–vis spectra of the reaction supernatants after the oxidation reaction were also tested and didn't find the characteristic absorption bands of manganese porphyrin moiety or related decomposition products, which also proved no degradation was occurred in the oxidation reaction.

3.2. Analysis of polymerization process

3.2.1. Appropriate ratio of reactants

The proper theoretical molar ratios of porphyrin to *p*-phenylenediamine should be 1:2 in porphyrin polymerization. With different ratios tested, the polymer had yield of 89% and BET surface area of 345 m^2g^{-1} at 1:2.5. The yield was slightly higher than that at 1:4 molar ratio, but its surface area was as low as 73 m^2g^{-1} (Table 1).

Table 1
Reactant ratios influenced the BET surface areas of the polymers.

Entry	Ratio[a]	Polymer Yield (%)	S_{BET} ($m^2\ g^{-1}$)
1	1:2	82	280
2	1:2.5	89	345
3	1:3	87	258
4	1:4	90	73

[a] Molar ratios of porphyrin to *p*-phenylenediamine.

3.2.2. Solvent, base and temperature screening for MnP-AMP synthesis

We initially focused on optimization of conditions for the coupling reaction of MnP-AMP. Some preliminary studies revealed that the best result was obtained with KOt-Bu as base and m-xylene as solvent at 135 °C. Temperature, base and solvents affected the reaction results evidently. Aromatic compounds containing benzene ring were significantly superior to other solvents (Table 2, entries 1–7). For example, the yield of MnP-AMP, which was very low with 1, 4-dioxane and DMF as solvents (23%, 19%, Table 2, entries 1, 2), reached over 49% when toluene and xylene were used. On the other hand, the yield of MnP-AMP was susceptible to temperature changes. Increasing the temperature from 110 °C to 135 °C elevated the yield from 51% to 89% (Table 2, entries 4, 7). Therefore, we chose m-xylene with a higher boiling point as solvent in order to appropriately raise the reaction temperature. Besides, base was also an important factor in reaction. Various bases affected the reaction depending on the basic strength and solubility in related solvent. KOt-Bu perfectly suited the reaction system due to suitable alkalinity and solubility. Cs_2CO_3, CsF and K_2CO_3 led to low yields (67%, 43%, 36%, Table 2, entries 8, 9, 10), and even no reaction occurred when KOH was used as base (Table 2, entry 11).

Table 2
Solvent, base and temperature screening for MnP-AMP synthesis.

Entry	Solvent	Base	Temp. (°C)	Yield (%)
1	Dioxane	KOt-Bu	110	23
2	DMF	KOt-Bu	110	19
3	Toluene	KOt-Bu	110	53
4	*m*-Xylene	KOt-Bu	110	51
5	*p*-Xylene	KOt-Bu	110	49
6	*o*-Xylene	KOt-Bu	110	50
7	*m*-Xylene	KOt-Bu	135	89
8	*m*-Xylene	Cs_2CO_3	135	67
9	*m*-Xylene	CsF	135	43
10	*m*-Xylene	K_2CO_3	135	36
11	*m*-Xylene	KOH	135	–[a]

[a] No reaction product.

3.3. Catalytic oxidation of alcohol

In the presence of isobutyraldehyde, aerobic oxidation of alcohol was well catalyzed with MnP-AMPs, producing the corresponding aldehyde under mild condition in acetonitrile (Table 3) and the mainly by-products of the oxidation reaction was the corresponding carboxylic products by GC–MS detection.

The three polymers with different specific surface areas showed markedly different catalytic performances (Table 3). When benzyl alcohol was employed as the substrate, polymer S_{345} had the best catalytic performance, achieving complete conversion within 2.0 h and aldehyde selectivity of 98%. The conversion and aldehyde

Table 4
S_{345} catalyzed oxidation of alcohols to aldehydes.[a]

Entry	Alcohol	Product	Time (h)	Conversion (%)	Aldehyde selectivity (%)
1	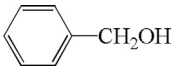	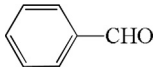	2.0	100	98
2	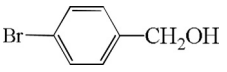	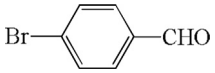	1.7	100	95
3	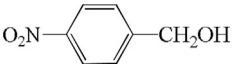	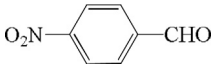	1.7	100	95
4	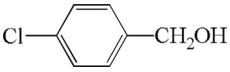	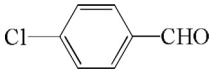	1.7	100	96
5	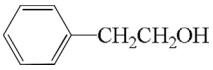	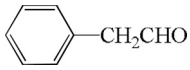	2.7	100	93
6	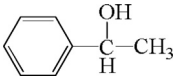	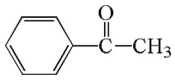	4.0	85	100
7	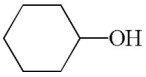	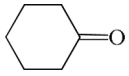	4.5	80	100
8	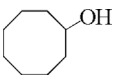	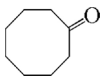	6.0	77	100
9	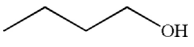	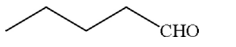	1.7	95	99
10	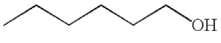	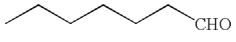	1.7	93	100
11	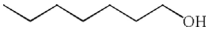	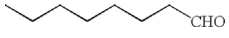	2.0	93	100

[a] Reaction condition: 3.0 mmol of benzyl alcohol, catalyst: MnP-AMP (S_{345}), Mn^{2+}/benzyl alcohol = 1/130000 (molar ratio), 9.0 mmol of isobutyraldehyde, air flow: 150 mL/min, solvent: 6 mL of acetonitrile, temperature: 40 °C.

Table 3
Effect of different catalysts on catalytic oxidation of benzyl alcohol to benzaldehyde.[a]

Entry	Catalyst	Time (h)	Conversion (%)	Aldehyde selectivity (%)
1	S_{345}	2.0	100	98
2	S_{258}	2.7	100	95
3	S_{73}	4.0	87	92
4	T(p-Br)PPMnCl	1.7	100	73

[a] Reaction condition: 3.0 mmol of benzyl alcohol, catalyst: Mn^{2+}/benzyl alcohol = 1/130000 (molar ratio), 9.0 mmol of isobutyraldehyde, air flow: 150 mL/min, solvent: 6 mL of acetonitrile, temperature: 40 °C.

selectivity of S_{73} were 87% and 92% respectively after 4.0 h. Also exhibiting high catalytic activity as a homogeneous catalyst, T(p-Br)PPMnCl completely converted benzyl alcohol into benzaldehyde in 1.7 h, but the aldehyde selectivity was only 73%.

With surface area of 345 m^2g^{-1}, MnP-AMP S_{345} had excellent catalytic performance for aromatic alcohol oxidation under mild conditions, nearly completely converting most of them (Table 4, entries 1–5) into corresponding aldehydes in 2.0 h. Furthermore, MnP-AMP also well catalyzed the oxidation of 1-benzyl alcohol to acetophenone, and cycloalkanol to cycloalkanone (Table 4, entries 6–8). Simple aliphatic primary alcohols such as methanol, ethanol and propyl-alcohol can't react in the oxidation reaction even the reaction temperature was increased to the boiling points. When the C number in the substrate was more than four, the aliphatic primary alcohols began to react under mild condition (Table 4, entries 9–11). The conversion rates were lower than that of benzyl alcohol compounds but with a higher selectivity for the aldehyde. For example, the conversion rate of *n*-butyl alcohol and the aldehyde selectivity were 95% and 99% after 1.7 h respectively (Table 4, entries 7). Similar to that, with the C number in the substrate increased, the conversion rate was a little reduced and the selectivity for the aldehyde always about 100%. C—N bonds in MnP-AMP increased the polarity of polymers and facilitated them to bind alcohol molecules.

MnP-AMP could be easily recycled after reaction by centrifugation, filtration, desiccation, or other simple separation methods. After 5 cycles, MnP-AMP had a recovery rate of more than 90%. Meanwhile, the recovered catalyst remained highly active under the optimized conditions. For example, the conversion rates of benzyl alcohol remained 98%, 95% and 91% respectively in three catalytic reactions, and the selectivity for the aldehyde has no obvious changed as 98%, 96% and 96% respectively in three catalytic reactions.

4. Conclusion

In conclusion, a N-containing heterocyclic carbene palladium complex $(Pd(IMes)Cl_2)_2$ was synthesized and applied to the N-arylation reaction in which metalloporphyrin and *p*-phenylenediamine were used as substrates. We synthesized a series of metalloporphyrin conjugated polymers MnP-AMPs with different surface areas under different conditions. Target products were obtained when the reaction was catalyzed by solvent m-xylene and base KOt-Bu with 1:2.5 porphyrin/p-phenylenediamine molar ratios at 135 °C. BET, SEM and TEM characterizations showed that the catalytic performance for alcohol oxidation of MnP-AMPs was boosted with increasing specific surface area. The pores were mainly diametered 1.27 nm, and MnP-AMP had an obvious lamellar structure, further composing a stereoscopic columnar structure. In the catalytic oxidation experiment, the selectivity of benzaldehyde was up to 98% and the conversion of benzyl alcohol was 100%. Besides exhibiting high catalytic oxidation activity against alcohols, MnP-AMP was also easily recyclable and reusable. Hence, MnP-AMP is an excellent heterogeneous catalyst for aerobic oxidation of alcohol as an eligible substitute for corresponding metalloporphyrin.

Acknowledgement

The authors thank the National Natural Science Foundation of China (Grant No. 21576074) for financial support.

Appendix A. Supplementary data

Supplementary data associated with this article can be found, in the online version, at http://dx.doi.org/10.1016/j.apcata.2016.02.003.

References

[1] J.T. Groves, T.E. Nemo, R.S. Myers, J. Am. Chem. Soc. 101 (1979) 1032–1033.
[2] M.L. Merlau, W.J. Grande, S.T. Nguyen, J. Hupp, J. Mol. Catal. A: Chem. 156 (2000) 79–84.
[3] L.H.R. Susana, M.M.Q. Simões, M.G.P.M.S. Neves, J.A.S. Cavaleiro, J. Mol. Catal. A: Chem. 201 (2003) 9–22.
[4] F. Adam, W.T. Ooi, Appl. Catal. A: Gen. 445 (2012) 252–260.
[5] V. Mirkhani, S. Tangestaninejad, M. Moghadam, Z. Karimian, Bioorg. Med. Chem. Lett. 13 (2003) 3433–3435.
[6] A.M. Machado, F. Wypych, S.M. Drechesel, S. Nakagaki, J. Colloid Interface Sci. 254 (2002) 158–164.
[7] G. Huang, Sh Y. Liu, Y.A. Guo, A.P. Wang, J. Luo, C.C. Cai, Appl. Catal. A: Gen. 358 (2009) 173–179.
[8] S.A. Hassan, H.A. Hassan, K.M. Hashem, H.M.A. Dayem, Appl. Catal. A: Gen. 300 (2006) 14–23.
[9] C.C. Guo, G. Huang, X.B. Zhang, C.G. Dong, Appl. Catal. A: Gen. 247 (2003) 261–267.
[10] G. Huang, A.P. Wang, Sh Y. Liu, Y.A. Guo, H. Zhou, Sh K. Zhao, Catal. Lett. 114 (2007) 174–177.
[11] A. Krivokapic, A.R. Cowlew, H.L. Anderson, J. Org. Chem. 68 (2003) 1089–1096.
[12] A. Modak, J. Mondal, A. Bhaumik, Appl. Catal. A: Gen. 459 (2013) 41–51.
[13] H.J. Mackintosh, P.M. Budd, N.B. Mckeown, J. Mater. Chem. 18 (2008) 573–578.
[14] I. Beletskaya, V.S. Tyurin, A.Y. Tsivadze, R. Guilard, C. Stem, Chem. Rev. 109 (2009) 1659–1713.
[15] S.J. Langford, C.P. Woodward, CrystEngComm 9 (2007) 218–221.
[16] A. Falber, L. Todaro, I. Goldberg, M.V. Favilla, C.M. Drain, Inorg. Chem. 47 (2008) 454–467.
[17] T. Soltner, M. Kuil, P.W.N.M.V. Leeuwen, J.N.H. Reek, J. Am. Chem. Soc. 128 (2006) 11344–11345.
[18] S.J. Lee, J.T. Hupp Coordin, Chem. Rev. 250 (2006) 1710–1723.
[19] N. Aratani, A. Osuka, Chem. Commun. 34 (2008) 4067–4069.
[20] R.W. Wagner, T.E. Johnson, J.S. Lindsey, J. Am. Chem. Soc. 118 (1996) 11166–11180.
[21] L. Chen, Y. Yang, Z. Guo, D. Jiang, Adv. Mater. 23 (2011) 3149–3154.
[22] Z. Wang, S.W. Yuan, A. Mason, B. Reprogle, D.J. Liu, L.P. Yu, Macromolecules 45 (2012) 7413–7419.
[23] S. Anderson, H.L. Anderson, J.K.M. Sanders, J. Chem. Soc. Perkin Trans. 1 (18) (1995) 2247–2254.
[24] L. Chen, Y. Yang, D. Jiang, J. Am. Chem. Soc. 46 (2010) 2653–2663.
[25] N. Marion, S.P. Nolan, Acc. Chem. Res. 40 (2008) 1440–1449.
[26] M.S. Viciu, R.M. Kissling, E.D. Stevens, S.P. Nolan, Org. Lett. 4 (2002) 2229–2231.
[27] A.D. Alder, F.R. Long, F.K. Kampos, J. Inorg. Nucl. Chem. 32 (1970) 2443–2445.